


**AUTHOR QUERY FORM**

 <b>ELSEVIER</b>	<b>Journal:</b> HE  <b>Article Number:</b> 12613	<b>Please e-mail or fax your responses and any corrections to:</b>  <b>E-mail:</b> <a href="mailto:corrections.essd@elsevier.tnq.co.in">corrections.essd@elsevier.tnq.co.in</a>  <b>Fax:</b> +31 2048 52789
--	--	---

Dear Author,

Please check your proof carefully and mark all corrections at the appropriate place in the proof (e.g., by using on-screen annotation in the PDF file) or compile them in a separate list. Note: if you opt to annotate the file with software other than Adobe Reader then please also highlight the appropriate place in the PDF file. To ensure fast publication of your paper please return your corrections within 48 hours.

For correction or revision of any artwork, please consult <http://www.elsevier.com/artworkinstructions>.

Any queries or remarks that have arisen during the processing of your manuscript are listed below and highlighted by flags in the proof.

<b>Location in article</b>	<b>Query / Remark: Click on the Q link to find the query's location in text Please insert your reply or correction at the corresponding line in the proof</b>
<b>Q1</b>	<p>Please confirm that given names and surnames have been identified correctly.</p> <div data-bbox="304 1102 895 1281" style="border: 1px solid black; padding: 5px;"> <p>Please check this box or indicate your approval if you have no corrections to make to the PDF file</p> <div style="display: inline-block; border: 1px solid black; width: 40px; height: 20px; vertical-align: middle;"></div> </div>

Thank you for your assistance.



ELSEVIER

Available online at [www.sciencedirect.com](http://www.sciencedirect.com)

ScienceDirect

journal homepage: [www.elsevier.com/locate/he](http://www.elsevier.com/locate/he)

## Highlights

- High crystalline Zr-MOF with well-defined shape was prepared via modulated synthesis.
- It has improved ease of handling during filtration process with micro-sized crystals.
- It has higher thermo-stability and good stability in selected aqueous media.
- It has enhanced H<sub>2</sub> storage capacity against the reported results.

UNCORRECTED PROOF

21  
22  
23  
24  
25  
26  
27  
28  
29  
30  
31  
32  
33  
34  
35  
36  
37  
38  
39  
40  
41



ELSEVIER

Available online at [www.sciencedirect.com](http://www.sciencedirect.com)

ScienceDirect

journal homepage: [www.elsevier.com/locate/he](http://www.elsevier.com/locate/he)

## Short Communication

# Modulated synthesis of zirconium-metal organic framework (Zr-MOF) for hydrogen storage applications

Q1 Jianwei Ren<sup>a,\*</sup>, Henrietta W. Langmi<sup>a</sup>, Brian C. North<sup>a</sup>, Mkhulu Mathe<sup>a</sup>,  
Dmitri Bessarabov<sup>b</sup>

<sup>a</sup>HySA Infrastructure Centre of Competence, Materials Science and Manufacturing, Council for Scientific and Industrial Research (CSIR), PO Box 395, Pretoria 0001, South Africa

<sup>b</sup>HySA Infrastructure Centre of Competence, Faculty of Engineering, North-West University (NWU), P. Bag X6001, Potchefstroom 2520, South Africa

## ARTICLE INFO

## Article history:

Received 22 August 2013

Received in revised form

11 October 2013

Accepted 16 October 2013

Available online xxx

## Keywords:

Zirconium-metal organic frame-  
work

Modulated synthesis

Hydrogen storage

Nucleation rate

## ABSTRACT

A modulated synthesis of Zr-metal organic framework (Zr-MOF) with improved ease of handling and decreased reaction time is reported to yield highly crystalline Zr-MOF with well-defined octahedral shaped crystals for practical hydrogen storage applications. The Zr-MOF obtained from the modulated synthesis showed high thermal and moisture stabilities with enhanced hydrogen storage capacity. Further study suggests that the modulated synthesis of Zr-MOF may lead to the development of a flow-through synthesis process.

Copyright © 2013, Hydrogen Energy Publications, LLC. Published by Elsevier Ltd. All rights reserved.

## 1. Introduction

With the discovery and exploration of various hydrogen storage materials, the implementation of efficient ways to prepare and process the materials for practical applications remains an engineering challenge. Research over the past decade has revealed the considerable potential for hydrogen storage applications of microporous metal organic frameworks (MOFs) with high surface areas and micropore volumes. However,

most MOFs, in particular zinc-based MOFs, are moisture-sensitive, and the structural decomposition leads to poor reproducibility of the materials and decreased hydrogen sorption capacity [1,2]. Additionally, the moisture sensitivity of MOFs poses a limitation on further handling towards commercial hydrogen storage applications, e.g. shaping of MOFs powder materials into application-specific configurations.

Interestingly, Cavka et al. [3] reported zirconium-based MOFs with comparable surface area to Zn-based MOFs (e.g.

\* Corresponding author. Tel.: +27 128412967; fax: +27 128412135.

E-mail address: [JRen@csir.co.za](mailto:JRen@csir.co.za) (J. Ren).

0360-3199/\$ – see front matter Copyright © 2013, Hydrogen Energy Publications, LLC. Published by Elsevier Ltd. All rights reserved.

<http://dx.doi.org/10.1016/j.ijhydene.2013.10.087>

MOF-5), and high structural resistance against water and external mechanical pressure. Therefore, these zirconium-based MOFs can be handled conveniently in atmospheric moisture. Compared to Zn-based MOFs, the enhanced stability of Zr-based MOFs can be attributed to their stronger Zr–O bonds relative to the Zn–O bonds (in Zn-based MOFs) within the secondary building unit (SBU) and to a high degree of interlinking of these SBUs [4]. Octahedral shaped crystals of Zr-MOF in the nanosize range (150–200 nm) have been synthesized after a crystallization time of 72 h [5]. However, as stated by Zhao et al. [5] synthesized Zr-MOF samples reported in the literature have usually exhibited morphologies comprising irregular inter-grown microcrystalline polyhedra, due to the difficulty to generate Zr-MOF of a regular crystalline morphology [6]. Our laboratory has also experienced some difficulties in the synthesis of Zr-MOF to obtain satisfactory crystals by following the reported synthetic procedures. These

difficulties were either the Zr-MOF precipitated as micro-sized aggregates of nanocrystals, or the synthesis that led to disordered phases with a low specific surface area and low hydrogen uptake capacity. In addition, the filtration process was time-consuming and the lab-scale centrifugation unable to effectively handle large volumes of solutions. Kitagawa et al. [7,8] demonstrated a coordination modulation approach for MOFs synthesis which prompted to the investigation of the modulated Zr-MOFs synthesis in our lab towards Zr-MOF products of improved reproducibility and crystallinity.

In this paper, we report the investigation of a fast modulated synthesis of micron-sized Zr-MOF material using formic acid as a modulator. The characterizations results showed that the use of formic acid was successful in the fast modulated synthesis of micron-sized Zr-MOF. The synthesized Zr-MOF products were reproducibly made with a high yield plus also a relatively higher crystallinity in a much shorter

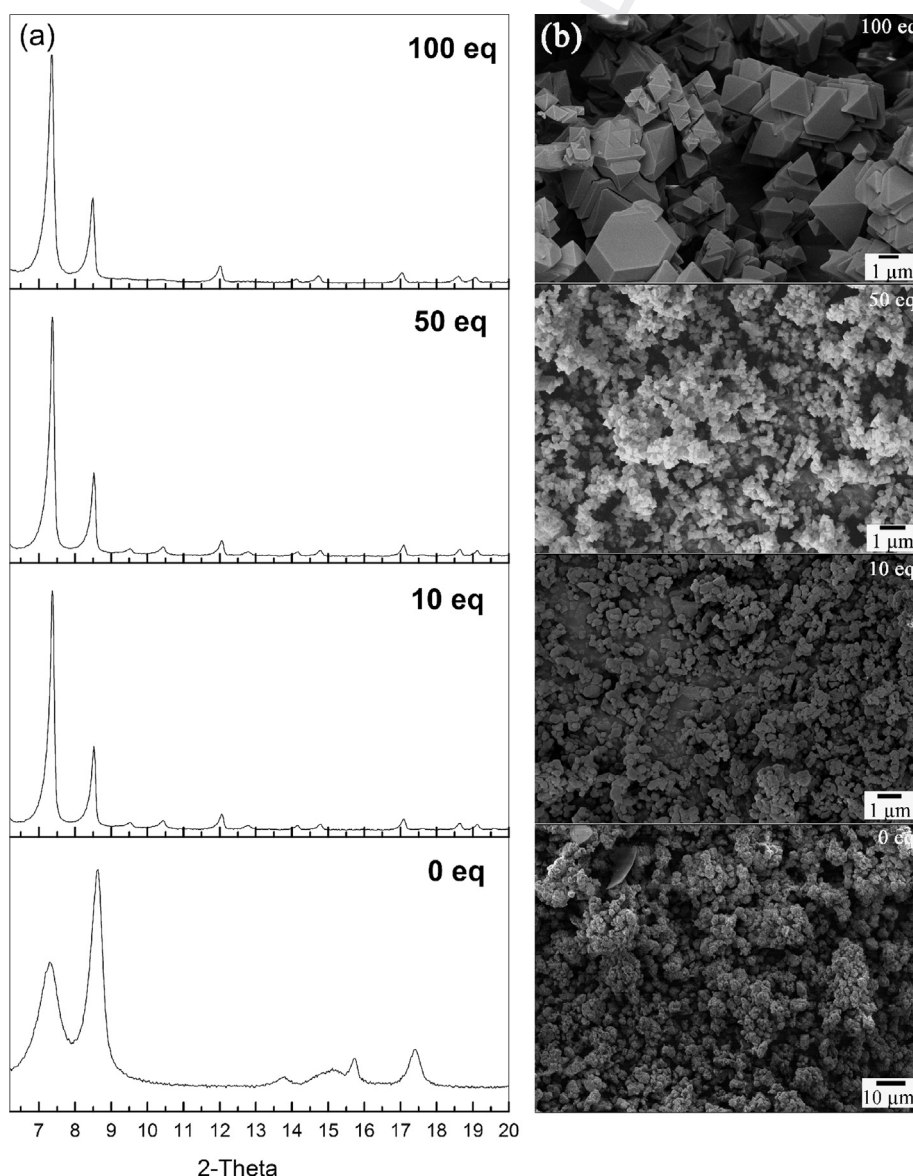


**Fig. 1 – (a) PXRD patterns and (b) SEM images of the obtained Zr-MOFs samples using formic acid as modulator in different equivalents with respect to  $ZrCl_4$ .**

reaction time of 2 h. Larger crystals sizes could be obtained with longer reaction time. The resultant Zr-MOFs also had high stability in several selected aqueous media, high thermal stability, and comparable specific surface area and hydrogen storage capacities to reported values in the literature.

## 2. Materials and methods

### 2.1. Reagents and chemicals

Zirconium tetrachloride ( $\text{ZrCl}_4$ , Sigma-Aldrich, 99.5+%), terephthalic acid (Sigma-Aldrich, 98%), N,N-dimethylformamide (DMF, Sigma-Aldrich, 99.8%), formic acid ( $\text{HCOOH}$ , Sigma-Aldrich, 95+%) and dried acetone (Sigma-Aldrich, 99.8+%) were purchased and used without further purification.

### 2.2. Up-scaled synthesis of Zr-MOF samples

The synthesis of Zr-MOFs was based on a previously reported procedure [9] with some amendments. Experiments were conducted using a 5000 ml round-bottom flask and a Heat-on 5000 ml Block from Heidolph to provide constant reaction temperature. In a typical procedure, 35.6 g (0.22 mol) of terephthalic acid and 51.3 g (0.22 mol) zirconium tetrachloride were ultrasonically dissolved in 2000 ml of DMF solvent. To gain a better understanding of the influence of the modulator, different equivalents of formic acid with respect to  $\text{ZrCl}_4$  were added. For the safety purposes, the outlet of flask was capped by a thick-walled balloon before being heated up to 120 °C and maintained at that temperature for 24 h under static conditions. After cooling, the product was collected by centrifugation or filtration, depending on the actual condition. The obtained white product was transferred into a drying apparatus with 100 ml dried acetone, and ultrasonically washed for 30 min. Then the solid was re-collected and dried under vacuum at room temperature. Furthermore, several parallel reactions were carried out at different reaction times (1–24 h) to monitor the nucleation rate of the specific synthesis.

### 2.3. Characterization

X-ray diffraction (XRD) patterns were obtained at room temperature by using a PANalytical X'Pert Pro powder diffractometer with Pixcel detector using Ni-filtered Cu- $K_\alpha$  radiation (0.154 nm) in the range of  $2\theta = 1\text{--}90^\circ$ , and scanning rate of  $0.1\text{ s}^{-1}$ . The exposure time of sample to environment was about 20 min including the sample preparation and testing procedure. An Auriga Cobra Focused-Ion Beam Scanning Electron Microscope (FIB-SEM) was used to study the morphology of the Zr-MOF samples. All the samples were mounted on a carbon tape and coated with gold prior to measurement. Thermal stability of obtained Zr-MOFs was checked by a thermogravimetric analysis (TGA) instrument (Mettler, Toledo, TGA/SDTA 851<sup>e</sup>). 10 mg of Zr-MOF sample was loaded into a pan and heated to 1000 °C at a rate of  $10\text{ }^\circ\text{C}/\text{min}$ . The air gas flow was maintained at 10 mL/min.

Surface area and pore characteristics measurements were carried out on an ASAP 2020 HD analyzer (Micromeritics) using

$\text{N}_2$ , and the BET surface areas were obtained from the linear region of the  $\text{N}_2$  isotherms using the two consistency criteria suggested in the literature [10–12].

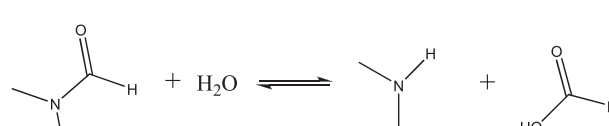
Volumetric  $\text{H}_2$  adsorption isotherms at 77 K and up to 1 bar were also measured on the ASAP 2020 instrument. All gas sorption isotherms were obtained using ultra-high purity grade (99.999%) gas. Before analysis, the pre-treated MOF samples (0.2–0.3 g) were outgassed in the analysis tube under vacuum (down to  $10^{-7}$  bar) with heating up to 200 °C, which is sufficient to remove solvent molecules without thermal decomposition or loss of framework crystallinity.

## 3. Results and discussion

In this section, the term equivalent (eq) refers to the molar ratio between formic acid and  $\text{ZrCl}_4$  in a synthesis batch. For example, in a synthesis designated as “100 eq”, the molar ratio of formic acid/ $\text{ZrCl}_4$  is 100:1.

PXRD patterns and the corresponding SEM images of the Zr-MOF products obtained using 0, 10, 50 and 100 eq of formic acid are shown in Fig. 1. Similar to other MOF materials, the relative intensity of the reflection peaks normally gives qualitative information of the crystals [13]. Without the addition of formic acid (0 eq synthesis), the intensity of the first reflection peak at  $2\theta = 7.4^\circ$  was low relative to the second peak at  $2\theta = 8.5^\circ$ , and the peaks were broader, indicating a low crystallinity phase, which was also confirmed by the corresponding SEM image showing ill-defined crystal shapes with agglomeration. With the addition of 10 eq of formic acid to the synthesis, the degree of crystallinity was significantly enhanced. When 50 eq of formic acid was used, all of the crystals began to take an octahedral shape with particle size around 100 nm. In the presence of 100 eq formic acid the obtained Zr-MOF crystals undoubtedly showed an octahedral shape with sharp edges and clearly visible facets. The crystal sizes were in the range of 1–3  $\mu\text{m}$ . The degree of agglomeration decreased with increasing equivalent of formic acid. Further evidence of decreased agglomeration was observed in the filtration process which was relatively fast. The PXRD patterns for 10, 50 and 100 eq synthesis showed the full set of reflections of a crystalline phase, and seven typical signals positioned at  $2\theta = 7.4, 8.5, 14.1, 14.7, 17, 18.6$  and  $19.1^\circ$  confirmed the successful synthesis of Zr-MOF (also known as UiO-66) [3].

The presence of formic acid in the synthesis obviously accelerated the formation of the crystalline Zr-MOF, with the highest equivalent of formic acid giving the largest crystals. During the synthesis of Zr-MOF, water is somehow essential for the hydrolysis of the Zr precursor including also for the oxygen supply for the formation of  $\text{Zr}_6\text{O}_4(\text{OH})_4(\text{O}_2\text{C})_{12}$  SBUs. N,N-dimethylformamide, however, easily absorbs water and decomposes as follows [6,14]:



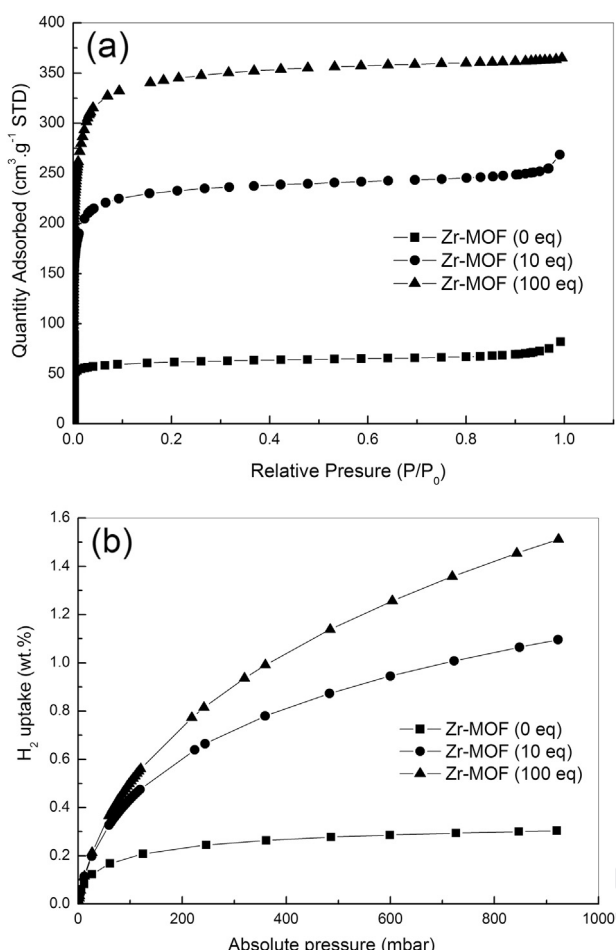


**Fig. 2 – (a) N<sub>2</sub> sorption isotherms, and (b) H<sub>2</sub> sorption isotherms at 77 K and 1 bar for the desolvated Zr-MOF samples obtained from 0, 10 and 100 eq syntheses.**

The presence of formic acid, added as a modulator, could displace this equilibrium to the left side to make more water available in the reaction system for the hydrolysis of the Zr precursor. By this indirect means, formic acid firstly sped up the formation of the SBUs and then accelerated the formation of the nuclei, and in the end the excess SBUs available around allowed nuclei to grow into larger crystals.

The nitrogen adsorption isotherm at 77 K of desolvated Zr-MOF powder samples obtained from 0, 10 and 100 eq syntheses were observed as a Type I isotherm (Fig. 2a), indicating a structure with micropores [15]. Table 1 lists the physical properties and H<sub>2</sub> uptake capacities of the Zr-MOF samples obtained in this work, and reported values in the literature. The Langmuir surface area determined from the sorption isotherm for the samples from 0, 10 and 100 eq syntheses are 273, 1032 and 1581 m<sup>2</sup> g<sup>-1</sup>, respectively, and that for Zr-MOF (100 eq) sample is larger than the reported value of 1187 m<sup>2</sup> g<sup>-1</sup> for UiO-66 [16]. The BET surface area and total pore volumes also increased from 241 m<sup>2</sup> g<sup>-1</sup> and 0.13 cm<sup>3</sup> g<sup>-1</sup> for the (Zr-MOF, 0 eq) in relation to the 1367 m<sup>2</sup> g<sup>-1</sup> and 0.56 cm<sup>3</sup> g<sup>-1</sup> (Zr-MOF, 100 eq), respectively.

The H<sub>2</sub> adsorption isotherms for the desolvated Zr-MOF samples from 0, 10 and 100 eq syntheses are shown in Fig. 2b. The H<sub>2</sub> storage capacity of Zr-MOF (0 eq) is quite low as 0.3 wt.%. The H<sub>2</sub> storage capacity of 1.1 wt.% for Zr-MOF (10 eq) sample compares quite well with the value in a patent reported by Hafizovic et al. [17], measured by the volumetric method at 77 K and pressure up to 1 bar. Due to the direct relationship between hydrogen capacity and the specific surface area of materials under the condition of 77 K and approximately 1 bar [18], Zr-MOF (100 eq) sample showed a relatively higher H<sub>2</sub> storage capacity of 1.5 wt.% as expected, resulting from a better crystallinity and higher BET surface area as discussed above.

Weight loss profiles from thermogravimetric analysis (TGA) tests showed that both of the as-prepared Zr-MOF samples from 10 to 100 eq syntheses present mainly two stages in weight loss (Fig. 3). A nearly continuous mass loss up to 350 °C was observed in the TGA plots. This mass loss probably corresponds to the removal of all organic material, including the evaporation of guest molecules from the pores such as solvent DMF and acetone. Between 350 and 500 °C the weight loss was almost linear indicating the high thermal stability of the Zr-MOFs. The TGA profile of Zr-MOF sample (10 eq) agreed very well with that UiO-66 originally reported by Cavka et al. [3]. Both Zr-MOFs maintained their structure up to 500 °C and after that a sudden weight loss was observed, which was attributed to decomposition of the Zr-MOFs to ZrO<sub>2</sub>. This suggests that modulated synthesis produces highly crystalline Zr-MOFs with high thermal stability.

**Table 1 – Comparison of physical properties and H<sub>2</sub> uptake capacities of the Zr-MOF samples reported in the literature.**

Sample	Size <sup>a</sup>	S <sub>BET</sub> (m <sup>2</sup> g <sup>-1</sup> ) <sup>b</sup>	Pore vol. (cm <sup>3</sup> g <sup>-1</sup> ) <sup>c</sup>	Micropore vol. (cm <sup>3</sup> g <sup>-1</sup> ) <sup>d</sup>	H <sub>2</sub> uptake (wt.%) <sup>e</sup>	Ref.
UiO-66	200 nm	1080	—	—	1.28	[3]
UiO-66	150–200 nm	1358	—	—	1.49	[5]
UiO-66	100 nm	1434	0.65	0.43	1.6	[9]
UiO-66	200 nm	1020	—	—	1.24	[17]
Zr-MOF (0 eq)	100–200 nm	241	0.13	0.08	0.35	This work
Zr-MOF (10 eq)	100–200 nm	918	0.42	0.30	1.1	This work
Zr-MOF (100 eq)	1–3 μm	1367	0.56	0.44	1.5	This work

<sup>a</sup> SEM images.

<sup>b</sup> BET surface area.

<sup>c</sup> From H<sub>2</sub>-K analysis.

<sup>d</sup> From H<sub>2</sub>-K analysis.

<sup>e</sup> Absorbed at 77 K and pressure up to 1 bar.

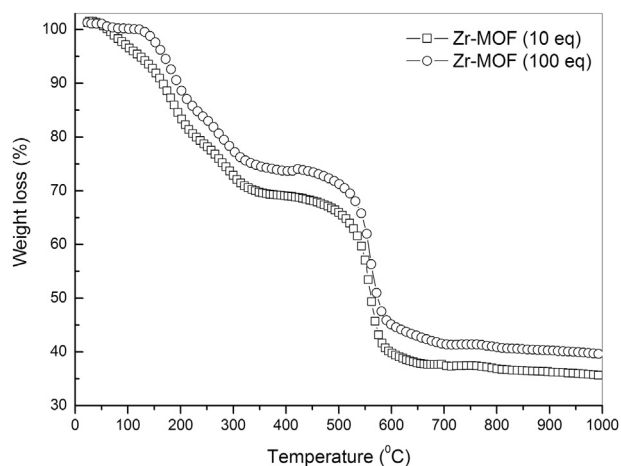


**Fig. 3 – Thermogravimetric analysis of the as-prepared Zr-MOF samples from 10 to 100 eq syntheses.**

Furthermore, a PXRD was used and is presented in Fig. 4a with a SEM (not shown here) to study nucleation rate in 100 eq synthesis. The results showed that high quality Zr-MOF crystals with well-defined octahedral shapes could be obtained within a reaction time of 2 h. The synthesized crystal sizes were in the range of 100–200 nm. With prolonged reaction time, Zr-MOF crystals larger sizes could be produced. These results directly demonstrate the possibility of continuous-flow Zr-MOF synthesis [19] and a subsequent transition to our targeted hydrogen storage applications. Further work is underway to develop a flow-through Zr-MOF synthesis process with high product yield and good product quality.

Once a powder adsorbent has been identified for hydrogen storage applications, the powder would need to be shaped for ease of handling, recyclability and prevention of potential pipeline contamination. Therefore the stability of Zr-MOF material (obtained from 100 eq synthesis) was tested in several potential binders, such as H<sub>2</sub>O, acetone, 25 wt.% glucose/H<sub>2</sub>O and 25 wt.% sucrose/H<sub>2</sub>O aqueous media. The Zr-MOF material from 100 eq synthesis was dispersed in each of the above-mentioned solutions and stirred at room temperature for 48 h. The PXRD patterns of the re-collected Zr-MOF samples did not indicate any sign of destruction or disorder in comparison to the as-prepared Zr-MOF powder (Fig. 4b). Therefore, the Zr-MOF material exhibited high stability in these aqueous media.

#### 4. Conclusions

The modulated synthesis of Zr-MOF material with excellent properties for practical hydrogen storage applications is reported. From the study of nucleation rates, highly crystalline Zr-MOF crystals in the size range of 100–200 nm with well-defined octahedral shape could be obtained in a decreased reaction time of 2 h. Larger size crystals could be obtained with prolonged reaction time. The synthesized product has potential to be up-scaled, with its coupled properties of high thermal and moisture stabilities. The product also exhibited

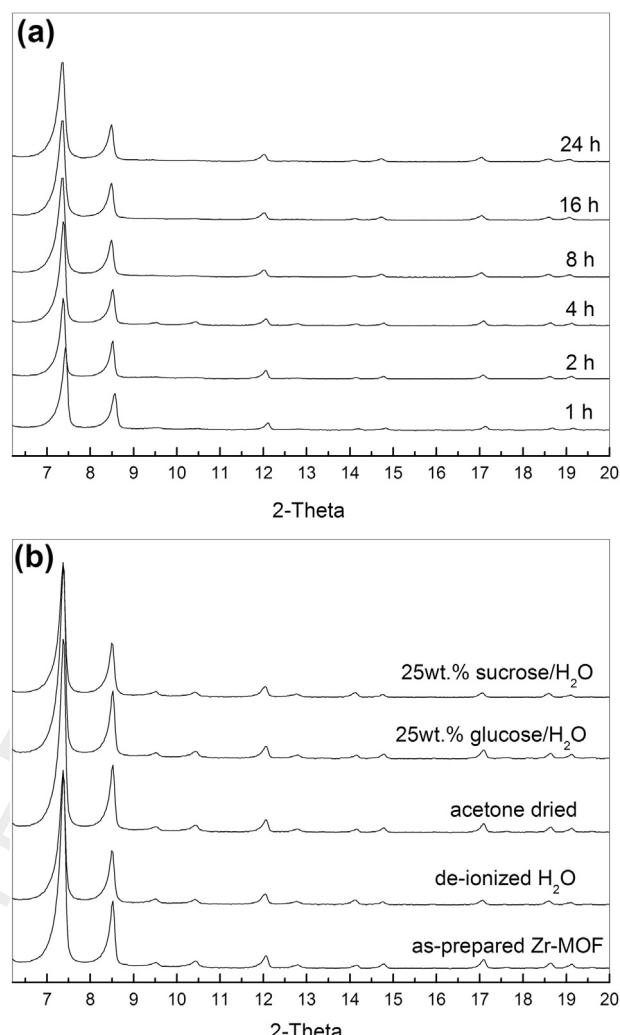


**Fig. 4 – PXRD patterns showing (a) Nucleation rate in 100 eq synthesis, and (b) stability of obtained Zr-MOF product (100 eq, 24 h) in selected aqueous media: H<sub>2</sub>O, acetone, 25 wt.% glucose/H<sub>2</sub>O and 25 wt.% sucrose/H<sub>2</sub>O (each stirred in different aqueous media for 48 h).**

comparable hydrogen storage properties of the obtained Zr-MOF samples thus making them promising for practical hydrogen storage applications.

#### Acknowledgements

This work was financially supported by the South African Department of Science and Technology (DST). The authors would like to thank Dr. Dave Rogers and Tshiamo Segakweng at the CSIR for collecting ASAP data.

#### REFERENCES

- [1] Kaye SS, Dailly A, Yaghi OM, Long JR. Impact of preparation and handling on the hydrogen storage properties of

- 1 Zn<sub>4</sub>O(1,4-benzenedicarboxylate)<sub>3</sub> (MOF-5). *J Am Chem Soc* 2007;129:14176–7. 33
- 2 [2] Nyuyen JG, Cohen SM. Moisture-resistant and 34
- 3 superhydrophobic metal-organic frameworks obtained via 35
- 4 postsynthetic modification. *J Am Chem Soc* 2010;132:4560–1. 36
- 5 [3] Cavka JH, Jakobsen S, Olsbye U, Guillou N, Lamberti C, 37
- 6 Bordiga S, et al. A new zirconium inorganic building brick 38
- 7 forming metal organic frameworks with exceptional 39
- 8 stability. *J Am Chem Soc* 2008;130:13850–1. 40
- 9 [4] Ebrahim AM, Levasseur B, Bandoz TJ. Interactions of NO<sub>2</sub> with 41
- 10 Zr-based MOF: effects of the size of organic linkers on NO<sub>2</sub> 42
- 11 adsorption at ambient conditions. *Langmuir* 2013;29:168–74. 43
- 12 [5] Zhao Q, Yuan W, Liang JM, Li JP. Synthesis and hydrogen 44
- 13 storage studies of metal-organic framework Uio-66. *Int J* 45
- 14 *Hydrogen Energy* 2013;38:13104–9. 46
- 15 [6] Schaate A, Roy P, Godt A, Lippke J, Waltz F, Wiebcke M, et al. 47
- 16 Modulated synthesis of Zr-based metal-organic frameworks: 48
- 17 from nano to single crystals. *Chem Eur J* 2011;17:6643–51. 49
- 18 [7] Tsuruoka T, Furukawa S, Takashima Y, Yoshida K, Isoda S, 50
- 19 Kitagawa S. Nanoporous nanorods fabricated by 51
- 20 coordination modulation and oriented attachment growth. 52
- 21 *Angew Chem Int Ed Engl* 2009;48:4739–43. 53
- 22 [8] Diring S, Furukawa S, Takashima Y, Tsuruoka T, Kitagawa S. 54
- 23 Controlled multiscale synthesis of porous coordination 55
- 24 polymer in nano/micro regimes. *Chem Mater* 2010;22:4531–8. 56
- 25 [9] Abid HR, Tian HY, Ang HM, Ang MO, Tade MO, Buckley CE, 57
- 26 et al. Nanosize Zr-metal organic framework (Uio-66) for 58
- 27 hydrogen and carbon dioxide storage. *Chem Eng J* 59
- 28 2012;187:415–20. 60
- 29 [10] Rouquerol J, Llewellyn P, Rouquerol F. Is the BET equation 61
- 30 applicable to microporous adsorbents? *Stud Surf Sci Catal* 62
- 31 2007;160:49–56. 63
- 32 [11] Bae YS, Yazaydin AÖ, Snurr RQ. Evaluation of the BET 64
- 33 method for determining surface areas of MOFs and zeolites 34
- 34 that contain ultra-micropores. *Langmuir* 2010;26:5475–83. 35
- 35 [12] Walton KS, Snurr RQ. Applicability of the BET method for 36
- 36 determining surface areas of microporous metal-organic 37
- 37 frameworks. *J Am Chem Soc* 2007;129:8552–6. 38
- 38 [13] Hafizovic J, Bjørgen M, Olsbye U, Dietzel PDC, Bordiga S, 39
- 39 Prestipino C, et al. The inconsistency in adsorption 40
- 40 properties and powder XRD data of MOF-5 is rationalized by 41
- 41 framework interpenetration and the presence of organic and 42
- 42 inorganic species in the nanocavities. *J Am Chem Soc* 43
- 43 2007;129:3612–20. 44
- 44 [14] Wißmann G, Schaate A, Lilienthal S, Bremer I, Schneider AM, 45
- 45 Behrens P. Modulated synthesis of Zr-fumarate MOF. 46
- 46 *Microporous Mesoporous Mater* 2012;152:64–70. 47
- 47 [15] Li H, Eddaoudi M, O’Keeffe M, Yaghi OM. Design and 48
- 48 synthesis of an exceptionally stable and highly porous 49
- 49 metal-organic framework. *Nature* 1999;402:276–9. 50
- 50 [16] Bácia PS, Guimarães D, Mendes PAP, Silva JAC, Guillerm V, 51
- 51 Chevreau H, et al. Reverse shape selectivity in the adsorption 52
- 52 of hexane and xylene isomers in MOF Uio-66. *Microporous* 53
- 53 *Mesoporous Mater* 2011;139:67–73. 54
- 54 [17] Hafizovic J, Olsbye U, Lillerud KP, Jacobsen S, Guillou N. Metal 55
- 55 organic framework compounds. *US* 2012/0115961 A1; May 10, 56
- 56 2012. 57
- 57 [18] Adams BD, Ostrom CK, Chen S, Chen AC. High-performance 58
- 58 Pd-based hydrogen spillover catalysts for hydrogen storage. *J* 59
- 59 *Phys Chem C* 2010;114:19875–82. 60
- 60 [19] Schoenecker PM, Belancik GA, Grabicka BE, Walton KS. 61
- 61 Kinetics study and crystallization process design for scale-up 62
- 62 of Uio-66-NH<sub>2</sub> synthesis. *AIChE J* 2013;59:1255–62. 63
- 63 64